

# *300 GHz microbolometer double-dipole antenna for focal-plane-array imaging*

*Leon Pavlovič\*, Janez Trontelj in Drago Kostevc*

*University of Ljubljana, Faculty of Electrical Engineering, Ljubljana, Slovenia*

**Abstract:** A room-temperature planar microbolometer double-dipole antenna for the focal-plane-array imaging at 300 GHz is presented. The fabricated antenna with a Titan bolometer consists of the full-wavelength parallel-dipole array on a thin nitride membrane, double impedance-transformation sections and low-pass-filter readout taps on a silicon substrate. The simulated antenna directivity at 300 GHz is about 11.7 dBi and agrees well with the measured radiation pattern. The radiation efficiency is about 85 % and the estimated bandwidth more than 200 GHz. A responsivity of 40 V/W and a noise-equivalent power of  $4 \times 10^{-11} \text{ W}/\sqrt{\text{Hz}}$  have been measured, respectively.

**Key words:** millimeter, terahertz, microbolometer antennas, sensors, focal-plane arrays

# *300 GHz mikrobolometriška antena z dvojnimi dipolom za slikanje s poljem v goriščni ravnini*

**Izvilleček:** Predstavljena je mikrobolometriška antena z dvojnimi dipolom za slikanje s poljem (senzorjev) v goriščni ravnini pri 300 GHz. Antena ima bolometer iz titana in sestoji iz celovalovnega dvojnega dipola, ki leži na tanki opni iz nitrída. Vsebuje še dvojno impedančno pretvorbo ter nizkopasovno sito z odcepnimi linijami na silicijevem substratu. Simulacijski rezultati, s smernostjo okoli 11,7 dBi, se dobro ujemajo z izmerjenimi smernimi diagrami. Sevalni izkoristek antene znaša okoli 85 %, ocenjena pasovna širina pa je približno 200 GHz. Izmerjena odzivnost je 40 V/W, ekvivalentna šumna moč (ang. »NEP«) pa  $4 \times 10^{-11} \text{ W}/\sqrt{\text{Hz}}$ .

**Ključne besede:** milimetrsko področje, teraherci, mikrobolometriška antena, senzori, polja v goriščni ravnini

\* Corresponding Author's e-mail: leon.pavlovic@fe.uni-lj.si

## *1. Introduction*

The research at millimeter-wave (mm-wave) and terahertz (THz) frequencies has been a continuous challenge for many decades and various applications, like radio astronomy, instrumentation, security, medicine, telecommunication, radar, etc. /1, 2/. For the mm-wave and THz sources (using either electrical, photonics or photo-conductive devices) and receivers the choice of an efficient antenna has been very applicative or device limited. Many antenna types, like the dipole, slot, spiral, bow-tie, log-periodic and horn, were successfully implemented at these frequencies /3, 4, 5, 6/. Due to its relatively simple manufacturing process and implementation, a planar antenna is a popular type. One of the most important limitations of a planar-antenna design is the choice of a suitable substrate, since it affects the antenna properties significantly. High-resistivity silicon (HR-Si) or indium phosphide (InP) substrates are typically the best choices, however (doped) silicon sub-

strate is also applicable or even desirable in some cases (suppression of unwanted resonances). The substrate thickness must be carefully chosen, otherwise surface waves in the substrate (for example,  $\text{TM}_0$  mode has a zero cut-off frequency) might have a major impact on the antenna performance (mostly reduced efficiency) when the substrate is thicker than approx.  $\lambda/50$  /7, 8, 9/. Often when a thick high-permittivity substrate is used, a large (typically HR-Si) lens is added underneath the substrate to couple the radiation through the substrate and lens /10/. For the focal-plane-array (FPA) imaging either a single lens or a lens array, i.e. fly's eye, can be used for the focusing of the received wave /8/. Another possibility is that the planar antenna is placed on a thin membrane with a ground plane distanced at  $\lambda/4$  from the antenna-structure metallization.

## 2. Antenna design

The antenna as an element of the receiving FPA imaging system must fulfill certain requirements: small crosstalk between adjacent antennas, low side lobes, small footprint, high efficiency, optimal impedance and radiation pattern, easy integration with the receiver electronics, etc. In our case the antenna directivity of about 12 dBi for each element was targeted to meet the required spatial resolution of the complete FPA using a large dielectric lens for the focusing.

A planar antenna on a thin membrane and a back-side metallization was chosen with the dipole as an antenna element. Simulation results proved that a 620  $\mu\text{m}$  long and a 40  $\mu\text{m}$  wide (full-wavelength) dipole in a free space (or on a thin membrane) is resonant at 300 GHz. A full-wavelength dipole was chosen over the half-wave dipole because of a higher directivity and higher impedance (approx. 500  $\Omega$  at resonance), respectively. Since the directivity of a single dipole is too small, a second dipole was added in parallel to form a dipole array. A double full-wavelength dipole antenna can have a symmetric radiation pattern, high directivity, high impedance (discussed later) and relatively simple manufacturing. The two dipoles are 612  $\mu\text{m}$  apart and are connected by a parallel transmission line (width/gap/width = 5/20/5  $\mu\text{m}$ ). The whole antenna structure with the detail of the realized load (Titan thermistor) is shown in Fig. 1 and one half of the antenna metallization in Fig. 2.

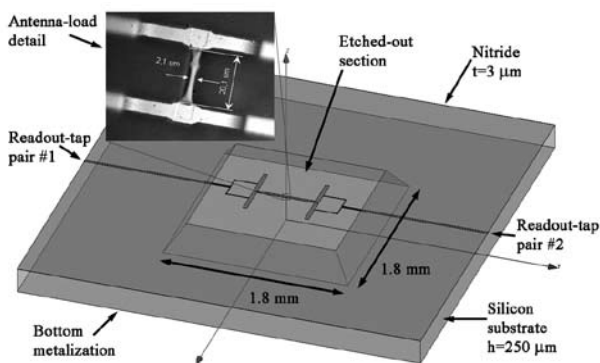


**Figure 1:** 300 GHz antenna structure with the realized antenna-load (thermistor) detail.

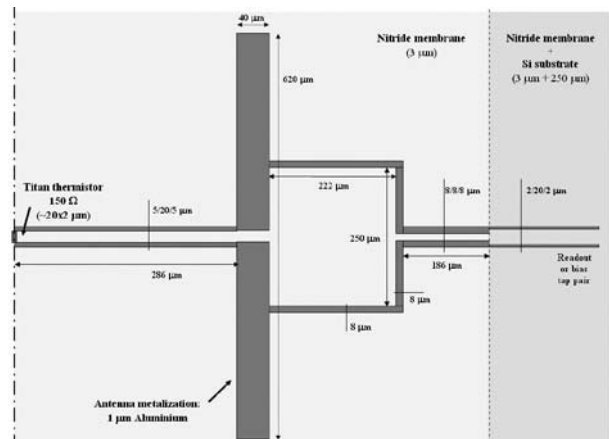


**Figure 2:** One half of the antenna metallization.

The double-dipole antenna lies on a thin (3  $\mu\text{m}$  thick) nitride membrane attached to a 250  $\mu\text{m}$  thick (doped) silicon substrate. A thin silicon dioxide membrane was also tested, but was found to be too fragile during the manufacturing process. During the manufacturing, the antenna metallization (1  $\mu\text{m}$  thick aluminum) on top of a thin nitride layer first lie on a bulk silicon substrate, which is later etched-out underneath the area of the antenna metallization. In this way an air pyramidal section (with the cross section of about  $1.8 \times 1.8 \text{ mm}^2$ ) is created below the two dipoles. Finally, the substrate with the membrane in the center is glued to a golden metallic plate (holder). The antenna cross section is shown in Fig. 3.

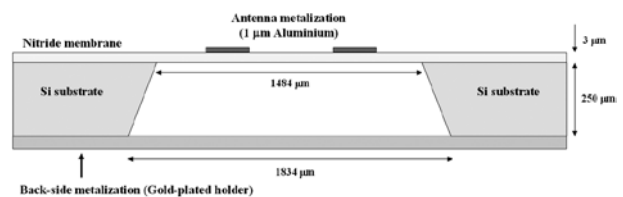


**Figure 3:** The antenna cross section.

The readout-tap pairs combine an impedance-transformation and low-pass sections, respectively, and are identical on both sides of the antenna. They are connected to the dipoles at a point of a maximal current (lowest impedance) at resonance. That is 125  $\mu\text{m}$  from the dipole's gap. In this way the readout and bolometer bias traces do not interfere with the antenna performance. The impedance transformation is done two times: firstly on the membrane and secondly on the membrane-to-substrate interface by an impedance change of the readout transmission lines. The low-pass section is implemented as a transmission line on a (lossy) silicon substrate. One readout-tap pair is used for the bolometer (thermistor) current bias and the other for the voltage readout, therefore the DC resistance of the antenna metallization does not

influence the low-frequency nor the DC measurements.

### 3. Measurements and results

The experimental setup included a 300 GHz transmitter and a receiver, comprising the double-dipole antenna as a detector and a lock-in amplifier for the readout and processing. The antenna load (thermistor as a bolometer) had a low-noise DC-current bias connected through one of the readout-tap pairs. The 300 GHz transmitter used was an experimental amplifier-multiplier-chain system (x24 frequency multiplication) delivering the output power of about 3-4 mW at 300 GHz out of the horn antenna. The multiplier chain has an operating frequency range of about 290 to 330 GHz and features an on-off modulation capability. The transmitter antenna is a rectangular horn with 26 dBi of gain. The lock-in amplifier and the transmitter's modulation input were driven synchronously at a frequency of 530 Hz. The antenna was fixed to a rotatable table and positioner stages for a precise position and orientation alignment. A close agreement is found between the simulated and the measured radiation patterns, which are shown in Fig. 4 and 5, respectively. For the numerical simulations the FEM (Ansoft HFSS) and the FDTD (CST MWS) solvers were used.

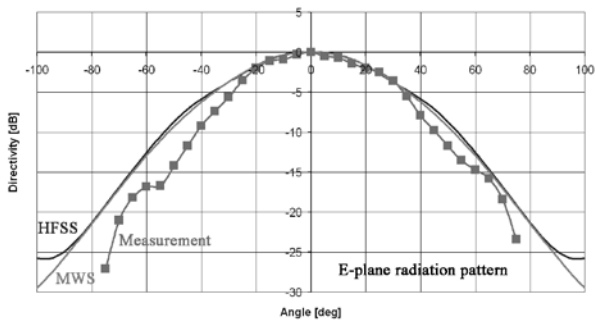


**Figure 4:** Measured and simulated E-plane radiation pattern at 320 GHz.

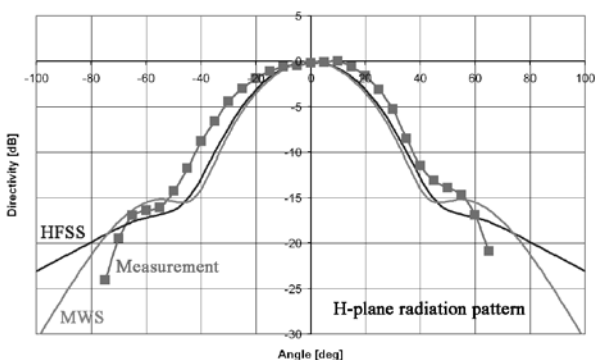


**Figure 5:** Measured and simulated H-plane radiation pattern at 320 GHz.

The numerically-computed directivity of the antenna is about 11.7 dBi at 85 % radiation efficiency. The simulated impedance of the antenna is  $100 + j40 \Omega$  at 300 GHz with the (full-wave) resonance at 280 GHz. The DC resistance of the realized Titan thermistor (20  $\mu\text{m}$  long and about 2  $\mu\text{m}$  thick) is  $150 \Omega$  and provides a relatively good match to the antenna impedance. A mismatch loss of about 1 dB was estimated. The responsivity of the microbolometer antenna was measured at 0.75 mA DC-current bias through the thermistor (bolometer). The distance between the transmitter and the receiver antenna was 110 mm. For the measured voltage of 48.4  $\mu\text{V}$  (by the lock-in amplifier) at 530 Hz modulation frequency a responsivity of 40 V/W was calculated.

The noise-equivalent power (NEP) was also estimated. The noise spectral density for the Titan  $150 \Omega$  thermistor used is about  $1.8 \times 10^{-9} \text{ V}/\sqrt{\text{Hz}}$ . Taking into consideration the responsivity of 40 V/W at 0.75 mA bias the NEP of  $4 \times 10^{-11} \text{ W}/\sqrt{\text{Hz}}$  is obtained. As a reference the NEP of  $5 \times 10^{-11} \text{ W}/\sqrt{\text{Hz}}$  was reported for the Golyay-cell detector [11]. The manufactured antenna was mounted onto a gold-plated multi-pin metal holder for an easy bonding and practical handling. A photograph of the antenna is shown in Fig. 6, where the antenna metallization on the membrane is clearly visible.

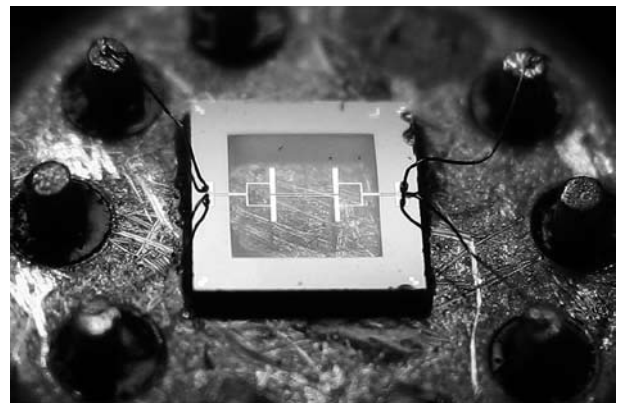


**Figure 6:** Photograph of the 300 GHz double-dipole antenna prototype mounted on a metal holder.

### 4. Conclusion

A 300 GHz room-temperature microbolometer double-dipole antenna for the FPA imaging has been fabricated. The antenna with a Titan bolometer consists of a full-wavelength dipole array on a 3  $\mu\text{m}$  thick nitride membrane, backed by a ground plane at a 250  $\mu\text{m}$  distance. Double impedance-transformation and low-pass-filter tap pairs on a silicon substrate are provided for the bias and readout, respectively. The measured radiation

patterns correspond well to the simulated patterns with the directivity of 11.7 dBi at the 85 % radiation efficiency at 300 GHz. The simulated antenna impedance at the feed point is about 100  $\Omega$ . Double filter-integrated tap pairs from the microbolometer antenna ensure optimal bolometer readout, since one tap pair provides the bolometer bias, while the other voltage readout. The antenna occupies an area of approx. 1.8x1.8 mm<sup>2</sup>. A responsivity of 40 V/W and a NEP of 4 x 10<sup>-11</sup> W/ $\sqrt$ Hz have been measured. Further improvements of the antenna will include a thin-film Bismuth bolometer, a vacuum encapsulation of the antenna structure and finally an active sensor/detector for a heterodyne receiver. Until now, a commercial lock-in amplifier has been used for the readout. Readout electronics is currently in development and will be later integrated with the antenna.

### *Acknowledgement*

Authors would like to thank Slovenian Ministry of Defence for the research funding. In addition we thank dr. Marijan Macek and other team members of Laboratory for microelectronics, Faculty of Electrical Engineering, University of Ljubljana, for manufacturing and testing of the antenna devices and also for many fruitful discussions.

### *References*

- 1 GOLDSMITH, P. F., HSIEH, C.-T., HUGUENIN, G. R., KAPITZKY, J., and MOORE, E. L.: 'Focal plane imaging systems for millimeter wavelengths', IEEE transactions on microwave theory and techniques, Vol. 41, No. 10, October 1993, pp. 1664-1675.
- 2 SIEGEL, P. H.: 'Terahertz technology', IEEE transactions on microwave theory and techniques, Vol. 50, No. 3, March 2002, pp. 910-928.
- 3 SIEGEL, P. H., DE MAAGT, P., and ZAGHLOUL, A. I.: 'Antennas for terahertz applications', IEEE antennas and propagation society international symposium, July 2006, pp. 2383-2386.
- 4 REBEIZ, G. M.: 'Millimeter-wave and terahertz integrated circuit antennas', Proceedings of the IEEE, Vol. 80, No. 11, November 2002, pp. 1748-1770.
- 5 FILIPOVIC, D. F., GEARHART, S. S., and REBEIZ, G. M.: 'Double-slot antennas on extended hemispherical and elliptical silicon dielectric lenses', IEEE transactions on microwave theory and techniques, Vol. 41, No. 10, October 1993, pp. 1738-1749.
- 6 FILIPOVIC, D. F., ALI-AHMAD, W. Y., and REBEIZ, G. M.: 'Millimeter-wave double-dipole antennas for high-gain integrated reflector illumination', IEEE transactions on microwave theory and techniques, Vol. 40, No. 5, May 1992, pp. 962-967.
- 7 ALEXOPOULOS, N. G., KATEHI, P. B., and RUTLEDGE, D. B.: 'Substrate optimization for integrated circuit antennas', IEEE transactions on microwave theory and techniques, Vol. MTT-31, No. 7, July 1983, pp. 550-557.
- 8 ROGERS, R. L., and NEIKIRK, D. P.: 'Use of broadside twin element antennas to increase efficiency on electrically thick dielectric substrates', International journal of Infrared and millimeter waves, Vol. 9, No. 11, 1988, pp. 949-969.
- 9 POZAR, D. M.: 'Considerations for millimeter wave printed antennas', IEEE transactions on antennas and propagation, Vol. AP-31, No. 5, September 1983, pp. 740-747.
- 10 YNGVESSON, S., GERECHT, E., NICHOLSON, J., RODRIGUEZ-MORALES, F., GU, D., ZHAO, X., WALDMAN, J., GOYETTE, T., and KOLLBERG, E.: 'Development of focal plane arrays with hot electron bolometer heterodyne detectors for 3 to 10 THz', IEEE Aerospace conference proceedings, 2004, pp. 724-734.
- 11 NAFTALY, M., DEAN, P., MILES, R. E., FLETCHER, J. R., and MALCOCI, A.: 'A simple interferometer for the analysis of terahertz sources and detectors', IEEE journal of selected topics in quantum electronics, Vol. 14, No. 2, March/April 2008, pp. 443-448.

Arrived: 24. 03. 2011

Accepted: 26. 1. 2012